

1786432

**INSTITUTO
DE FÍSICA**

preprint

IFUSP/P-217

EFFICIENCY FACTORS IN MIE SCATTERING

by

H.M. Nussenzveig and W.J. Wiscombe

National Center for Atmospheric Research
Boulder, Colorado 80307

B.I.F. - USP

UNIVERSIDADE DE SÃO PAULO
INSTITUTO DE FÍSICA
Caixa Postal - 20.516
Cidade Universitária
São Paulo - BRASIL

IFUSP/P 217
B.I.F. - USP

Efficiency Factors in Mie Scattering

H. M. Nussenzveig[†]

and

W. J. Wiscombe

National Center for Atmospheric Research^{††}

Boulder, Colorado 80307

April 1980

[†]Cooperative Institute for Research in the Environmental Sciences, Boulder, CO 80309 and NCAR. (Permanent address: Instituto de Fisica, Universidade de São Paulo, Brazil).

^{††}The National Center for Atmospheric Research is sponsored by the National Science Foundation.

ABSTRACT

Asymptotic approximations to the Mie efficiency factors for extinction, absorption and radiation pressure, derived from complex angular momentum theory and averaged over $\Delta\beta \sim \pi$ ($\beta =$ size parameter), are given and compared with the exact results. For complex refractive indices $N = n + i\kappa$ with $1.1 \leq n \leq 2.5$ and $0 \leq \kappa \leq 1$, the relative errors decrease from $\sim 1-10\%$ to $\sim 10^{-2}-10^{-3}\%$ between $\beta = 10$ and $\beta = 1000$, and computing time is reduced by a factor of order β , so that the Mie formulae can advantageously be replaced by the asymptotic ones in most applications.

The efficiency factors for extinction (Q_{ext}), absorption (Q_{abs}) and radiation pressure (Q_{pr}) in Mie scattering¹ are basic quantities for the study of radiative transfer in planetary atmospheres (besides many other applications). Typically, droplet size parameters $\beta = ka$ ($k =$ wave number, $a =$ droplet radius) range from $\ll 1$ up to $\sim 10^4$, with complex refractive indices $N = n + ik$, $1.1 \lesssim n \lesssim 1.9$, $10^{-9} \lesssim k \lesssim 1$. The efficiencies vary extremely rapidly² with β , n and k ; one is usually interested in their averages $\langle Q \rangle$ over a size dispersion $\Delta\beta$.

Evaluation of the exact Mie expressions¹ requires summing $\sim \beta$ partial waves. In view of the wide range of parameters, this is often impractical even with the fastest computers available. Approximations¹ based on geometrical optics and classical diffraction theory do not have the required accuracy, even at the largest values of β (cf. below).

The complex angular momentum theory of Mie scattering³ leads to asymptotic expressions for the efficiency factors in the domain

$$\beta^{1/3} \gg 1 ,$$

$$|N^2 - 1|^{1/2} \beta^{1/3} / |N|^2 \gg 1 . \quad (1)$$

By a simple extension of previously developed techniques,^{4,5} we find for the extinction efficiency,

$$\begin{aligned}
Q_{\text{ext}} = & 2 + 1.9923861 \beta^{-2/3} + 8 \operatorname{Im} \left\{ \frac{1}{4} (N^2 + 1) (N^2 - 1)^{-1/2} \beta^{-1} \right. \\
& - N^2 (N + 1)^{-1} (N^2 - 1)^{-1} \left[1 + \frac{i}{2\beta} \left(\frac{1}{N-1} - \frac{N-1}{N} \right) \right] \beta^{-1} \exp[2i(N-1)\beta] \\
& \left. - \frac{1}{2} (N - 1) \sum_{j=1}^{\infty} \left[j - \left(\frac{N-1}{2} \right) \right]^{-1} \left(\frac{N-1}{N+1} \right)^{2j} \exp[2i(N - 1 + 2jN)\beta] \right\} \\
& - 0.7153537 \beta^{-4/3} - 0.3320643 \operatorname{Im} [e^{i\pi/3} (N^2 - 1)^{-3/2} (N^2 + 1) \\
& (2N^4 - 6N^2 + 3)] \beta^{-5/3} + O(\beta^{-2}) + \text{ripple}, \quad (2)
\end{aligned}$$

where the "ripple" is a quasi-periodic series of spikes with approximately zero average over an interval $\Delta\beta \sim \pi$.

To obtain the average absorption efficiency $\langle Q_{\text{abs}} \rangle$ over $\Delta\beta \sim \pi$, one applies the modified Watson transformation³ to the corresponding Mie series expansion,^{1,2} and one then takes the average over $\Delta\beta$. The result⁶ is

$$\langle Q_{\text{abs}} \rangle = \langle Q_{\text{abs}} \rangle_{\text{F}} + \langle Q_{\text{abs}} \rangle_{\text{a.e.}} + \langle Q_{\text{abs}} \rangle_{\text{b.e.}}, \quad (3)$$

$$\langle Q_{\text{abs}} \rangle_{\text{F}} = \sum_{\lambda=1}^2 \int_0^{\pi/2} \phi(r_{j\lambda}) \sin\theta \cos\theta \, d\theta, \quad (4)$$

$$\langle Q_{\text{abs}} \rangle_{\text{a.e.}} = 2^{-1/3} \beta^{-2/3} \sum_{\lambda=1}^2 \int_0^{x_a} \phi(r_{j\lambda}^+) \, dx, \quad (5)$$

$$\langle Q_{\text{abs}} \rangle_{\text{b.e.}} = 2^{-1/3} \beta^{-2/3} \sum_{\lambda=1}^2 \int_0^{x_b} [\phi(r_{j\lambda}^-) - \phi(\tilde{r}_{j\lambda}^-)] \, dx, \quad (6)$$

where

$$\phi(r_{j\lambda}) = (1 - e^{-b})(1 - r_{2\lambda}) / (1 - r_{1\lambda} e^{-b}), \quad (7)$$

and $r_{2\lambda}$, $r_{1\lambda}$ are, respectively, the external and internal reflectivities for polarization λ , given by

$$r_{j\lambda} = |R_{j\lambda}|^2 \quad (j, \lambda = 1, 2) ,$$

$$R_{j\lambda} = (-)^j (z_j - ue_\lambda)/(z + ue_\lambda) , \quad (8)$$

$$z = \cos\theta , \quad u = N \cos\theta' , \quad \sin\theta = N \sin\theta' , \quad (9)$$

$$e_1 = 1 , \quad e_2 = N^{-2} , \quad z_1 = z , \quad z_2 = \begin{cases} z & \text{for (4)} \\ z^* & \text{for (5), (6)} \end{cases}$$

and

$$b = 4\beta \operatorname{Im}(N \cos\theta' + \theta' \sin\theta) . \quad (10)$$

By (9), θ' is the complex angle of refraction corresponding to the angle of incidence θ . In (4), $r_{j\lambda}$ are the Fresnel reflectivities ($r_{2\lambda} = r_{1\lambda}$), and in (7) b is the damping exponent along a complex shortcut through the sphere. Thus (4) is an improved version of the geometrical-optic¹ result.

The remaining terms in (3) represent the contribution from the edge domain³ (a.e. = above edge; b.e. = below edge); $r_{j\lambda}^\pm$ is obtained from $r_{j\lambda}$ by the substitution

$$z \rightarrow z^\pm = -(2/\beta)^{1/3} e^{i\pi/6} [\ln \operatorname{Ai}(\pm x e^{2i\pi/3})] , \quad (11)$$

where Ai is the Airy function, x is related to θ by

$$\sin\theta = 1 \pm 2^{-1/3} \beta^{-2/3} x \quad (+ \text{ in a.e., } - \text{ in b.e.}) , \quad (12)$$

[with corresponding changes in the derived quantities (9), (10)], and

$$x_a = 2^{1/3} (n-1) \beta^{2/3}, \quad x_b = (\beta/2)^{2/3}. \quad (13)$$

Finally, in (6), $\tilde{r}_{j\lambda}^-$ is obtained from $r_{j\lambda}^-$ by the substitution

$$z^- \rightarrow \tilde{z}^- = (2/\beta)^{1/3} \sqrt{x}. \quad (14)$$

The average radiation pressure efficiency is given by⁶

$$\langle Q_{pr} \rangle = 1 - \langle wg \rangle_F - \langle wg \rangle_{a.e.} - \langle wg \rangle_{b.e.}, \quad (15)$$

$$\langle wg \rangle_F = \operatorname{Re} \sum_{\lambda=1}^2 \int_0^{\pi/2} d\theta \sin\theta \cos\theta e^{-2i\theta} [-|R_{2\lambda}|^2$$

$$+ |1 - (R_{2\lambda})^2|^2 (1 + f_2 |R_{1\lambda}|^2 e^{-b})^{-1} f_2 e^{-b}], \quad (16)$$

$$\langle wg \rangle_{a.e.} = 2^{-1/3} \beta^{-2/3} \operatorname{Re} \sum_{\lambda=1}^2 \int_0^{x_a} (\rho_\lambda^+ - \tau_\lambda^+ + 1) dx, \quad (17)$$

$$\langle wg \rangle_{b.e.} = 2^{-1/3} \beta^{-2/3} \operatorname{Re} \sum_{\lambda=1}^2 \int_0^{x_b} [(\rho_\lambda^- - \hat{\rho}_\lambda^-) - (\tau_\lambda^- - \hat{\tau}_\lambda^-)] dx, \quad (18)$$

where

$$\rho_\lambda = f_1(z) R_{2\lambda}^* R'_{2\lambda}, \quad (19)$$

$$\tau_\lambda = f_1(z) f_2 e^{-b} (1 + R_{1\lambda}^*) (1 + R'_{1\lambda}) (1 + R_{2\lambda}^*) (1 + R'_{2\lambda}) (1 + R_{1\lambda}^* R'_{1\lambda} f_2 e^{-b})^{-1}, \quad (20)$$

$$f_1(z) = (1 + iz^*) / (1 - iz), \quad f_2 = e^{-2i\theta'}, \quad (21)$$

$$R'_{j1} = (f_j)^{-1} [N^2 z_j - u + (-)^j iM^2] (N^2 z + u + iM^2)^{-1}, \quad (22)$$

$$R'_{j2} = (f_j)^{-1} [(N^2 + M^2) z_j - u + (-)^j iM^2(1 - uz_j)]^{-1} \quad (22)$$

$$= [(N^2 + M^2) z + u + iM^2(1 + uz)]^{-1}, \quad (23)$$

with $M^2 = N^2 - 1$. In all quantities with (\pm) upper indices, the substitutions (11) and (12) are understood. Finally, $\hat{\rho}_\lambda^-$ and $\hat{\tau}_\lambda^-$ are obtained from ρ_λ^- , τ_λ^- by the substitution

$$z^- \rightarrow \hat{z}^- = (2/\beta)^{1/3} (\sqrt{x} + i/4x). \quad (24)$$

Again, (16) represents an improved version of the geometrical-optic⁷ result, while the remaining terms in (15) represent above-edge and below-edge corrections.

In radiative transfer calculations, one employs instead of $\langle Q_{pr} \rangle$ the average asymmetry factor $\langle \overline{\cos\theta} \rangle$, where¹

$$\overline{\cos\theta} = (Q_{ext} - Q_{pr}) / (Q_{ext} - Q_{abs}). \quad (25)$$

The asymptotic expression for $\langle \overline{\cos\theta} \rangle$ therefore follows⁸ from our previous results.

We have made detailed comparisons⁶ between the exact Mie results (suitably averaged to eliminate the ripple⁹) and the above asymptotic approximations¹⁰ over the ranges $10 \leq \beta \leq 5000$, $0 \leq \kappa \leq 1$, for $n = 1.10, 1.33, 1.50, 1.90$ and 2.50 . Results for $n = 1.33$ and $10 \leq \beta \leq 1000$ are shown in Figure 1.

Figure 1a is a three-dimensional plot of $\langle Q_{ext} \rangle$. The oscillations arise from interference between diffracted and transmitted light, and they are damped out as $\kappa\beta$ increases. Figure 1b shows level curves for the logarithm of the percentage error of approximation

(2). Negative values (errors $< 1\%$) are shown by dotted lines. Thus the relative error falls below 1% already at $\beta \geq 15$, it is $\leq 0.1\%$ at $\beta \geq 70$, $\leq 0.01\%$ at $\beta \geq 200$ and $\leq 10^{-3}\%$ at $\beta \geq 10^3$.

Figures 1c and 1d show similar plots for $\langle Q_{\text{abs}} \rangle$, and Figures 1e and 1f for $\langle Q_{\text{pr}} \rangle$. The relative errors are somewhat greater than for $\langle Q_{\text{ext}} \rangle$ and are worst for $\langle Q_{\text{pr}} \rangle$, where one must have $\beta \geq 90$ to achieve better than 1% error. For $\langle \cos \theta \rangle$ (not shown), the accuracy is better than 1% for $\beta \geq 30$.

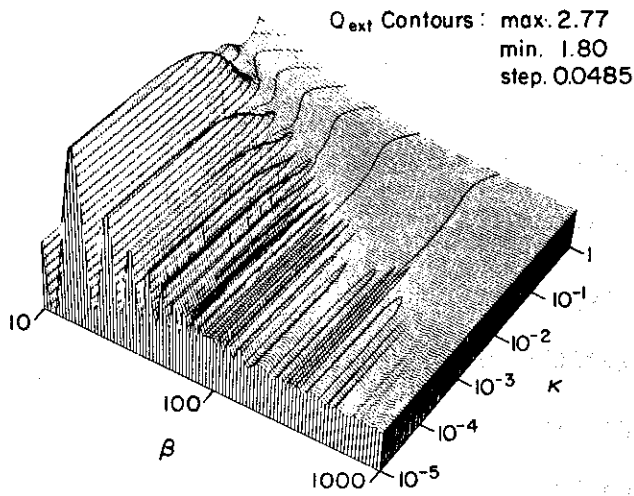
The accuracy improves not only as β increases, but also as n increases, in agreement with (1). Previously known approximations (based on geometrical optics and classical diffraction theory) have an accuracy that is almost independent of n and that only reaches 1% at $\beta = 1000$ and $0.2-0.5\%$ at $\beta = 5000$.

The computing time is reduced relative to Mie computations roughly by a factor of $O(\beta)$, and it is only about twice that for geometrical-optic approximations.

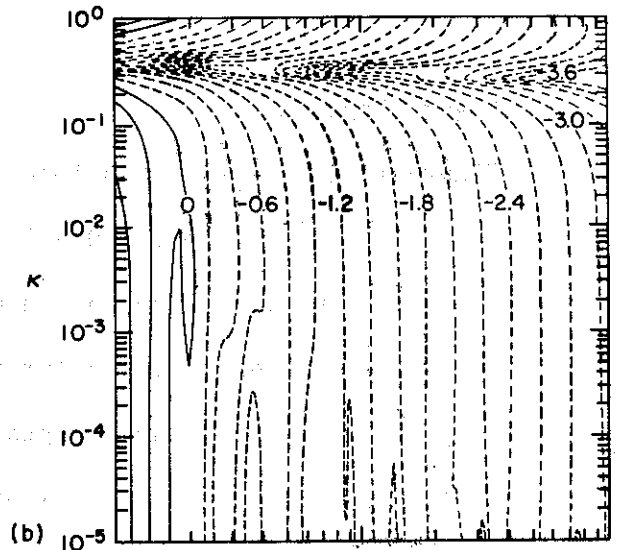
Besides the improvement to the geometrical-optic type contributions, the main asymptotic corrections arise from the edge domain. Their functional form is quite similar to the geometrical-optic one, extended to complex angles of incidence and refraction. Thus, as was found in previous discussions,³ the edge effects represent a kind of analytic continuation of ray optics to complex paths, where diffraction corresponds to barrier penetration. Similar interpretations have been suggested in atomic,¹¹ nuclear¹² and particle¹³ physics.

Figure Caption

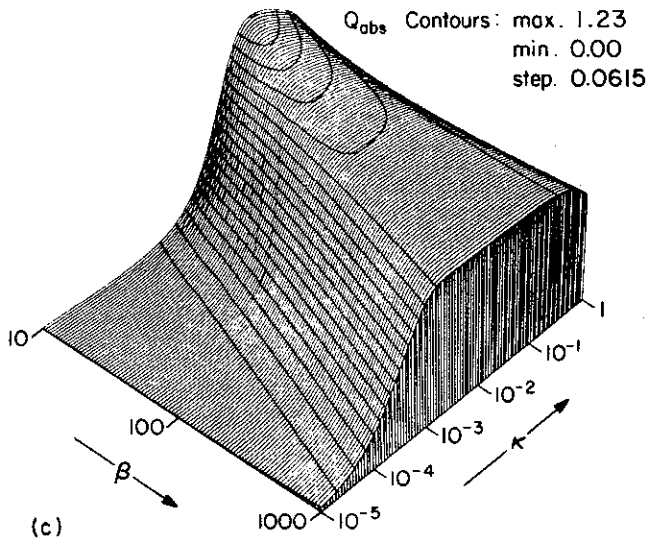
- Figure 1 (a) three-dimensional plot of $\langle Q_{\text{ext}} \rangle$ for $n = 1.33$, $10^{-5} \leq \kappa \leq 1$, $10 \leq \beta \leq 10^3$. The numbers attached to surface represent values of $\langle Q_{\text{ext}} \rangle$.
- (b) Level curves for the logarithm of the percentage errors of the asymptotic approximation to $\langle Q_{\text{ext}} \rangle$. Negative values (errors $< 1\%$) are shown by dotted lines.
- (c) Same as (a) for $\langle Q_{\text{abs}} \rangle$.
- (d) Same as (b) for $\langle Q_{\text{abs}} \rangle$.
- (e) Same as (a) for $\langle Q_{\text{pr}} \rangle$.
- (f) Same as (b) for $\langle Q_{\text{pr}} \rangle$.



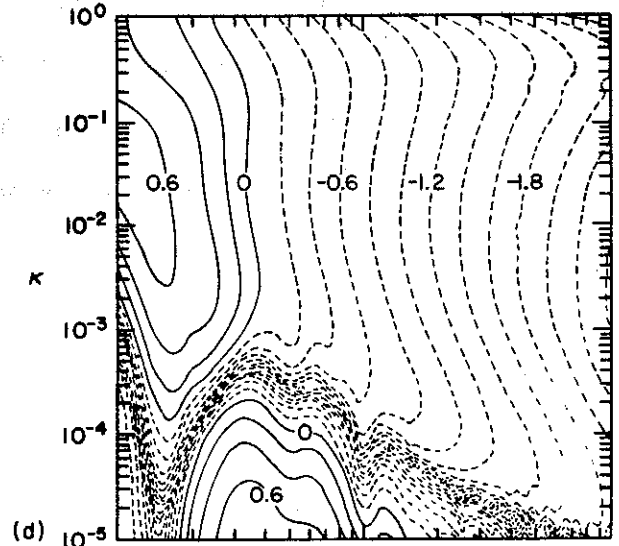
(a)



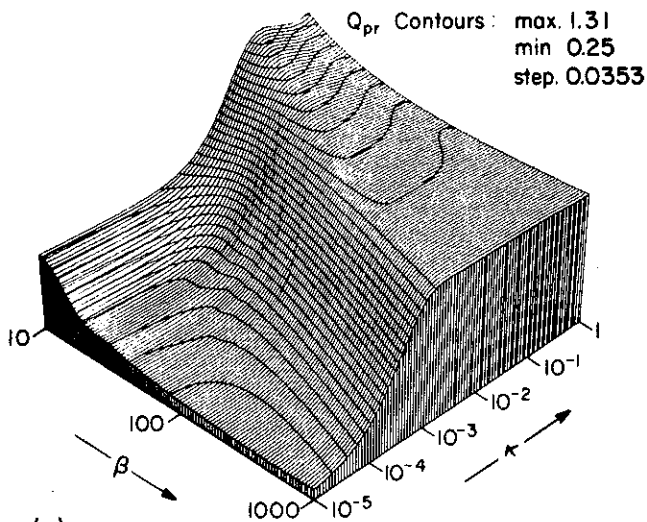
(b)



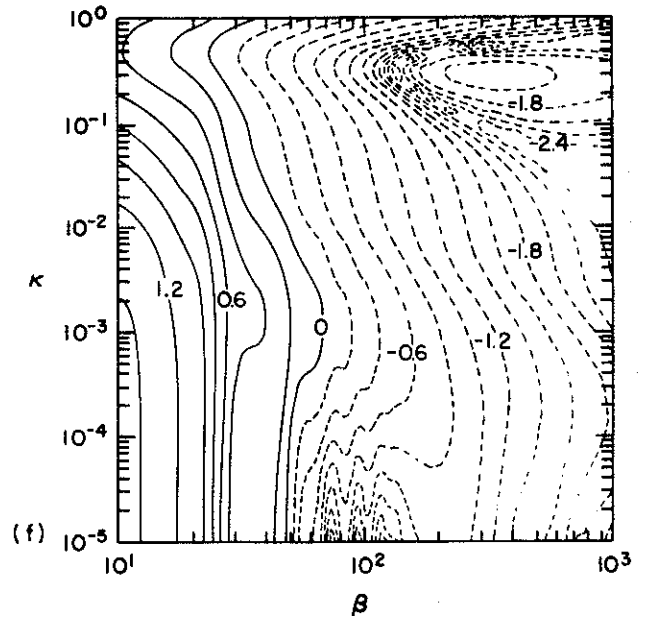
(c)



(d)



(e)



(f)

Footnotes

¹H. C. van de Hulst, Light Scattering by Small Particles (Wiley, New York, 1957).

²W. M. Irvine, J. Opt. Soc. Am. 55, 16 (1965).

³Cf. H. M. Nussenzveig, J. Opt. Soc. Am. 69, 1068 (1979) and references therein.

⁴H. M. Nussenzveig, J. Math. Phys. 10, 82,125 (1969).

⁵V. Khare, Ph.D. Thesis, University of Rochester (1975).

⁶H. M. Nussenzveig and W. J. Wiscombe, to be published.

⁷P. J. Debye, Ann. Physik 30, 57 (1909).

⁸It is a good approximation to substitute the average ratio in (25) by the ratio of averages.

⁹The Mie computations were performed using vector-speed algorithms developed by one of us (Wiscombe, Appl. Opt., May 1980). High-frequency ripple was removed from the Mie data by least-squares quartic spline fitting with knots every $\Delta\beta \sim 10$ for Q_{abs} and Q_{pr} , and by low-pass filtering for Q_{ext} .

¹⁰A fairly mature set of computer routines for calculating Eqs. 2, 3 and 15, including rational function fits to the requisite Airy function ratios, has been developed during the course of this research and is available from one of us (W.J.W.) upon request.

¹¹J. N. L. Connor and W. Jakubetz, Molec. Phys. 35, 949 (1978); S. Bosanac, *ibid.*, 1057.

¹²R. C. Fuller and P. J. Moffa, Phys. Rev. C15, 266 (1977).

¹³B. Schrempp and F. Schrempp, Phys. Lett. B70, 88 (1977); Preprint, CERN-TH 2573 (1978).